RSC Advances

PAPER

View Article Online
View Journal | View Issue

Check for updates

Cite this: *RSC Adv.*, 2025, **15**, 13031

Influence of LNA modifications on the activity of the 10–23 DNAzyme†

Marcelo Muñoz-González,[abc] Rodrigo Aguilar,[b] Adrian A. Moreno[c] and Marjorie Cepeda-Plaza *[a]

The 10–23 DNAzyme is a catalytic DNA molecule that efficiently cleaves RNA in the presence of divalent cations such as Mg^{2+} or Ca^{2+}. Following their discovery, the 10–23 DNAzymes demonstrated numerous advantages that quickly led them to be considered powerful molecular tools for the development of gene-silencing tools. In this study, we evaluate the efficiency of the 10–23 DNAzyme and an LNA-modified analog in cleaving human MALAT1, an RNA overexpressed in cancer cells. First, we perform *in vitro* assays using a 20 nt RNA fragment from the MALAT1 sequence, with 2 mM and 10 mM Mg^{2+} and Ca^{2+} as cofactors, to evaluate how LNA modifications influence catalytic activity. We found that the activity is increased in the LNA-modified DNAzyme compared to the unmodified version with both cofactors, in a concentration-dependent manner. Finally, the RNA-cleaving activity of the LNA-modified, catalytically active 10–23 DNAzyme was tested in MCF7 human breast cancer cells. We found that the DNAzyme persists for up to 72 h in cells and effectively silences MALAT1 RNA in a concentration-dependent manner as early as 12 h post-transfection.

Received 7th January 2025
Accepted 9th April 2025

DOI: 10.1039/d5ra00161g

rsc.li/rsc-advances

Open Access Article. Published on 23 April 2025. Downloaded on 4/15/2026 9:26:23 PM.
This article is licensed under a Creative Commons Attribution-NonCommercial 3.0 Unported Licence.

Introduction

The 10–23 DNAzyme, first discovered in 1997,[1–3] stands as one of the most characterized DNAzymes for catalytic DNA-based applications. This DNAzyme has been employed in gene silencing applications and has undergone testing in various clinical studies since 2009.[4–10] Recent efforts have concentrated on optimizing its design to enhance stability against nuclease attacks in the cellular environment and improve catalytic efficiency.[4,11–13]

The 10–23 DNAzyme, like other RNA-cleaving DNAzymes, is part of a group of biomolecular tools that have been explored for gene silencing. Interference RNA (siRNA), antisense oligonucleotides (ASOs) or CRISPR-Cas13 are traditional methods used for the same purpose.[14] Compared to these methodologies, DNAzymes offer some advantages[4,13] such as: (i) they can be obtained by simple and high-scale synthesis, (ii) they can be designed to target practically any RNA with high specificity through Watson and Crick pairing, making them adaptable to any required silencing application and (iii) they possess catalytic autonomy to cleave target RNAs, unlike the other techniques, which largely depend on proteins from the cellular machinery to cleave target RNAs.[15] These advantages, combined with the greater chemical stability of DNA compared to other biomolecules such as RNA or proteins, have prompted a growing number of investigations pursuing the application of RNA-cleaving DNAzymes as gene silencing tools.[16,17]

In the cellular environment, where nuclease activity could quickly degrade unmodified nucleic acids, the incorporation of unnatural chemical modifications is a common strategy to increase stability. Locked nucleic acids (LNAs)[18–22] have become a powerful tool in various nucleic acid-based therapies due to their ability to significantly improve the binding strength and stability against nucleolytic degradation, which is particularly beneficial in the context of gene silencing.[22–28] Besides, LNA-modified oligonucleotides are generally well tolerated in biological systems.[21]

Regarding the use of LNA in DNAzyme based applications, often one or more LNA modifications are located in the RNA binding regions in different types of arrangements.[12,22–26,29] Studies conducted by Schubert *et al.*[29] have shown that incorporation of 3 or 4 LNA modifications in the 5′ and 3′ ends of the 10–23 DNAzyme, increased the observed rate constant by ~13 times with 10 mM Mg^{2+} (50 mM Tris–HCl, pH 7.5 at 37 °C). Meanwhile, Wang *et al.*[12] have reached a ~3 times increment in the activity with 1 mM Mg^{2+} (50 mM Tris–HCl, pH 7.5 at 24 °C); however, at 10 mM Mg^{2+} the rate constant decreased by a factor of 0.78 times. Some studies include the chemical replacement in the catalytic core.[30,31] While modifications at certain positions within the core did not cause product inhibition, they led to a reduction in catalytic activity, likely because they hinder the

[a]*Chemical Sciences Department, Universidad Andres Bello, Santiago, Chile*
[b]*Institute of Biomedical Sciences, Faculty of Medicine and Faculty of Life Sciences, Universidad Andres Bello, Chile*
[c]*Centro de Biotecnología Vegetal, Facultad de Ciencias de la Vida, Universidad Andres Bello, Santiago, Chile. E-mail: marjorie.cepeda@unab.cl*

† Electronic supplementary information (ESI) available. See DOI: https://doi.org/10.1039/d5ra00161g

© 2025 The Author(s). Published by the Royal Society of Chemistry

Open Access Article. Published on 23 April 2025. Downloaded on 4/15/2026 9:26:23 PM. This article is licensed under a Creative Commons Attribution-NonCommercial 3.0 Unported Licence.

conformational flexibility needed for efficient catalysis.[32] It has been demonstrated that when one or more LNA modifications are included in a DNA:RNA duplex, the sugars in the DNA strands shift from a balance between S- and N-type conformations in the unmodified duplex to predominantly N-type when the modified nucleotides are incorporated.[33] Also, the introduction of the LNA-modified nucleotides causes significant conformational changes in the neighboring unmodified nucleotides of the DNA strand.

In addition, LNAs have shown to improve base pairing selectivity and RNA binding affinity, improving the ability of the DNAzyme to selectively bind to an specific target, which is especially important when working with long RNAs that often have highly structured regions.[34] However, their incorporation could also reduce the DNAzyme's multiple turnover ability due to high binding affinity, which hinders the dissociation of the cleaved substrate, therefore, limiting their therapeutic efficacy.[4]

In terms of its mechanism, the 10–23 DNAzyme efficiently accelerates the cleavage of an RNA sequence between a purine nucleotide and a pyrimidine (most effectively GU or AU)[35] in the presence of divalent metal ions, such as Mg^{2+}, Ca^{2+} or Mn^{2+}.[2,3] This DNAzyme consists of a 15-nucleotide catalytic loop, which is flanked by two substrate recognition regions of variable length at the 3′ and 5′ ends, called arms, which bind to the RNA substrate by Watson and Crick pairing (Fig. 1).[3] It has been established that the sequence or nucleotide composition of the DNAzyme arms can be designed to target any sequence of a target RNA (containing the GU or AU dinucleotide), without drastically affecting the activity of the DNAzyme. However, a recent report indicates that there is an influence of the nucleotides adjacent to the cleavable dinucleotide on the catalytic efficiency of the 10–23.[11]

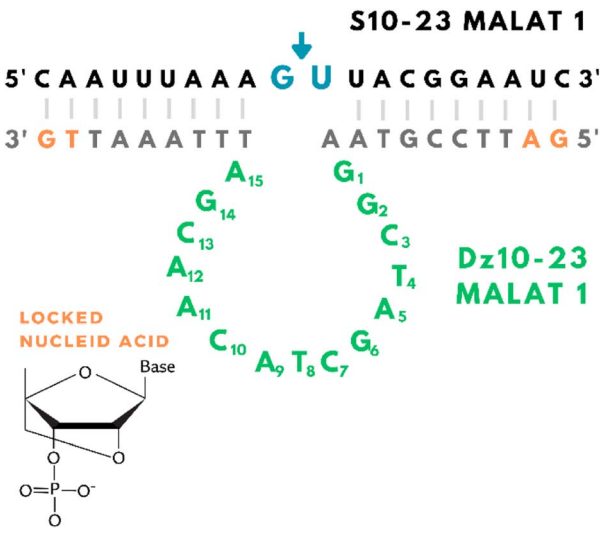

Fig. 1 Secondary structure of the 10–23 DNAzyme. The figure illustrates the RNA substrate strand in black, the substrate recognition strand of the DNAzyme in light gray. The two residues in light blue show the cleavage site. Catalytic core and numbering are shown in green. Orange bases indicate where LNA modifications were introduced in the DNAzyme sequence in this study.

The RNA cleavage catalyzed by the 10–23 DNAzyme follows a transesterification reaction, which is initiated by the nucleophilic attack of the 2′-OH group on the adjacent phosphate.[2] The reaction generates as products two RNA fragments with 2′,3′-cyclic phosphate and 5′-OH termini (Fig. S1†).[36] Recently, the solution structure of the 10–23 has been obtained by a combination of nuclear magnetic resonance (NMR), molecular dynamics simulations (MD) and electron paramagnetic resonance (EPR).[32] This assemble suggested a compacted core region, which includes an extra turn of the loop around the RNA. This arrangement would effectively immobilize the substrate, exposing the cleavage site (GU) entirely to the catalytic loop region. Also, three Mg^{2+} binding regions have been identified that can be related to structural scaffolding, activation, and catalysis.[37] This configuration would allow the in-line condition for the nucleophilic attack of the adjacent O2′ on the phosphate.

In addition, our group have recently provided functional evidence supporting the role of general acid–base catalysis in the mechanism of the 10–23.[38] By the comparison of the pH-rate profile of the 10–23 DNAzyme and a variant containing a 2-aminopurine modification at G14 we demonstrate the crucial role of G14 as a general base to activate the nucleophile during catalysis. Additionally, using Pb^{2+} as a cofactor, along with Mg^{2+}, we revealed that hydrated metal ions might act as general acids, stabilizing the 5′O leaving group.[38] These findings agree with the observations made by MD simulations.[37] While it is well known that chemical modifications are a valuable synthetic method to prevent nuclease degradation of DNAzymes in the cellular environment, their specific influence on the mechanism of the DNAzyme have not been investigated, which prevents the possibility to achieve a rational design of more stable and active variants for the development of *in vivo* applications.

In this study, we designed a 10–23 LNA variant to target a region of the human long non-coding RNA (lncRNA) MALAT1 (Metastasis-Associated Lung Adenocarcinoma Transcript 1), one of the most extensively studied nuclear lncRNAs due to its overexpression in different types of cancer [39]. In cancer cells, MALAT1 contributes to the cell survival through multiple mechanisms, leading to propose it as a therapeutic target.[40] In breast cancer cell lines, the transcript has been targeted with small molecules,[41] short interfering RNAs[42] and antisense oligonucleotides[43] leading to transcript degradation and reduced cell proliferation and metastasis.[42] In the last years, two studies have reported the use of 8–17 DNAzymes variants against murine MALAT1. Khani-Habibabadi *et al.* used 8–17 to reduce MALAT1 expression in rat oligodendrocyte precursor cells,[44] and Chiba *et al.* reported an 8–17 DNAzyme modified with xeno-nucleic acid that reduced MALAT1 expression in a mouse hepatoma Hepa1c1c7 cells.[45] So far, there are no studies reporting the use of 10–23 DNAzymes against human MALAT1 in human cells.[44]

In this study, we compare through activity assays, the influence of introducing two LNA modifications at each end of the substrate binding domain of the DNAzyme on the catalytic activity of the 10–23, using 2 mM and 10 mM Mg^{2+} and Ca^{2+} as

© 2025 The Author(s). Published by the Royal Society of Chemistry

Open Access Article. Published on 23 April 2025. Downloaded on 4/15/2026 9:26:23 PM. This article is licensed under a Creative Commons Attribution-NonCommercial 3.0 Unported Licence.

cofactors. While Ca^{2+} is not as commonly used as Mg^{2+} in DNAzyme catalysis, the choice to use Ca^{2+} alongside Mg^{2+} in our experiments allows for a deeper exploration of how these two cofactors influence DNAzyme performance. Both cations are critical for numerous cellular processes and exhibit an inverse regulatory relationship, where an increase in one ion typically suppresses the other. This dynamic regulation suggests that for DNAzymes utilizing both ions, at least one will generally be available to support their catalytic activity, making them suitable choices for our *in vitro* experiments.

Here we show that working under single turnover conditions; to isolate the catalytic step of the reaction, LNA modifications increased the observed rate constant with both Mg^{2+} and Ca^{2+}. The increment found is sharper when working with low concentrations of the divalent metal cofactor. Also, we show the effective silencing of human MALAT1 in MCF-7 breast cancer cells occupying DNAzyme 10–23 with the modification of LNA at various concentrations.

Experimental

10–23 sequences and its modified analogs, in addition to 5′-FAM labeled RNA substrate were obtained from Integrated DNA Technologies, Inc. (Coralville, IA). All other chemicals were of at least ACS reagent grade and were purchased from either Sigma-Aldrich or Bio-Rad.

Sequence design

We targeted a region of human MALAT1 previously identified as accessible to an LNA GapmeR antisense oligonucleotides (ASOs) designated g#9. [46] This ASO targeted a region around nucleotide 3820 of the MALAT1 intronless variant (Genbank: NR_002819.5). To fulfill the requirements for a consecutive GU nucleotide at the center,[35] the RNA substrate used for *in vitro* experiments corresponded to nucleotides 3806–3825 (designated as S10-23-MALAT1 in Table 1, GU in bold). This sequence is also present in spliced MALAT1 variants 2 (NR_144567.1; nucleotides 4879–4898) and 3 (NR_144568.1; nucleotides 4636 to 4655). The substrate was covalently labeled with a FAM at the 5′ end. The 10–23 DNAzyme variant was designed with a recognition sequence (named arms) of 9 nucleotides complementary to the substrate where the guanine is free and the uracil is complemented, the catalytic region is composed of 15 nucleotide and was based on the sequence reported in the literature.[12,29] Additionally, a DNAzyme sequence containing 2 LNA (locked nucleic acid) chemical modifications in each of the 3′ and 5′ ends was introduced to improve the DNAzyme cellular stability, since it has been shown this modification increases the resistance against endonucleases degradation and the affinity for a complementary sequence.[19] The position of LNA modifications was inspired in results found by Schubert *et al.*[29] and Wang, *et al.*[12] An inactive analogue of 10–23 was used as control for cellular studies. In this construct, the thymine located in position 4 of the catalytic loop was change by a C to abolish activity completely.[47] All sequences are detailed in Table 1.

In vitro activity assays

All activity assays were carried out at 37 °C under single-turnover conditions with 10 μM enzyme and 1 μM substrate, in a buffer containing 50 mM TRIS and 100 mM $NaNO_3$, pH 7.5. The buffer was incubated with Chelex 100 resin to remove trace metal ion impurities. The sample solution containing the enzyme and substrate in buffer was denatured at 70 °C in a water bath for 1 minute and then annealed by gradually cooling the container to room temperature. After annealing the solution, a 2 μL aliquot was added to 15 μL of stop solution containing 8 M urea, 50 mM EDTA, 1× TBE. This was the 'zero-point' control before the initiation of the reaction. There-after, 5 μL of $MgCl_2$ and $CaCl_2$ solutions were added to the sample to initiate the reaction. 19.2 mM and 96 mM metal stock solutions were used to achieve final concentrations of 2 and 10 mM, respectively. Later, 5 μL aliquots were taken at suitable time intervals and added to 15 μL of stop solution to end the reaction. A denaturing 20% polyacrylamide gel was used to separate the substrate from the product. Gel imaging was performed on the gel doc system XRQ G:Box Chemi (Synegen) and quantified with the Genesys Tools software. The percentage of product at time 't' was calculated by taking the ratio of the 5′-cleaved product to the total substrate (cleaved product plus the uncleaved substrate). Kinetic plots were created and fitted using Origin 8.5 software (OriginLab Corporation, Northampton, MA) according to the eqn (1):

$$P = \%P_0 + \%P_\infty(1 - e^{-k \cdot t}) \quad (1)$$

where $\%P_0$ is the initial amount of product (at time, $t = 0$), $\%P_\infty$ is the amount of product formed at the endpoint plus the initial amount of product of the reaction (at $t = \infty$), P is the amount of product at time t, and k is the observed constant rate. All

Table 1 DNA and RNA sequences used in this study. All sequences are displayed from 5′ to 3′. + indicates LNA-modified nucleotide. The thymine mutated by a C in the LNA modified variant used as inactive control is indicated in red

Name	Sequence
S10-23-MALAT1	5′-CAAUUUAAA**GU**UACGGAAUC-3′
Dz10-23-MALAT1	5′-GATTCCGTAA**GGCTAGCTACAACGA**TTTAAATTG-3′
LNA-Dz10-23-MALAT1	5′-+G+ATTCCGTAA**GGC**T**AGCTACAACGA**TTTAAAT+T+G-3′
FAM-LNA-Dz10-23-MALAT1	5′-FAM-**T**+G+ATTCCGTAAGGCTAGCTACAACGATTTAAAT+T+G-3′

Open Access Article. Published on 23 April 2025. Downloaded on 4/15/2026 9:26:23 PM. This article is licensed under a Creative Commons Attribution-NonCommercial 3.0 Unported Licence.

reported values are the average of at least three independent trials.[48]

Dependence of activity on divalent metal ions concentration

The rate of DNA-catalyzed RNA cleavage was assayed under single-turnover conditions in the presence of Mg^{2+} and Ca^{2+}, at pH 7.5 and 37 °C. The curves are fitted with the eqn (2):

$$k_{obs} = \frac{k_{max} \cdot [M^{2+}]}{K_D + [M^{2+}]} \quad (2)$$

where k_{max} is rate constant in the presence of saturating divalent metal cation and K_D is the apparent dissociation constant for the divalent metal cation.[2,49] Derivations of eqn (1) and (2) are described in the ESI.†

MCF7 cell line culture

Experiments with cells were conducted using the human breast cancer cell line MCF7 (ATCC: HTB-22), which grows attached to plastic wells. Cells were cultured in a humidified incubator (5% CO_2, 37 °C) in Dulbecco's Modified Eagle's Medium supplemented with 10% (v/v) fetal bovine serum and 100 U per mL penicillin–streptomycin (all reagents from Thermo Fisher Scientific).

Transfection of DNAzymes

Transfection of DNAzymes to MCF7 cells was performed using Lipofectamine 3000 (Thermo Fisher Scientific) according to the manufacturer's instructions. DNAzyme variants were added at concentration ranging from 0.5 to 4 μM. Both active and inactive DNAzyme variants were tested. After transfection, cells were incubated for 12 h, 24 h, or 48 h until subsequent experiments.

Cell counting

To determine the number of cells growing in a well, cells incubated with DNAzyme variants, or the inactive variant used as control for 24 h or 48 h were detached using 0.25% trypsin–EDTA (Thermo Fisher Scientific). An aliquot of the cell suspension was mixed 1 : 1 with trypan blue dye and loaded into an improved Neubauer chamber (Marienfeld, Germany). Live cells (which did not incorporate the dye) were counted under an optical microscope. The total number of cells per well was determined using the eqn (3):

$$\text{Number of cells in the well} = (\text{cells in one } 0.1\ \text{mm}^3 \text{ quadrant}) \times (\text{dilution factor}) \times 10\,000 \times (\text{volume of cell suspension in mL}) \quad (3)$$

RNA purification and quantification of gene expression

Cells incubated with DNAzymes or the inactive variant used as control for 12 h, 24 h or 48 h were lysed directly by adding TRIzol to the well (Thermo Fisher Scientific). Lysates were then subjected to the Direct-zol RNA Miniprep purification kit protocol (Zymo Research). Purified RNA was quantified using a Nanodrop instrument (Thermo Fisher Scientific), and 1 μg was used for reverse transcription with SuperScript IV Reverse Transcriptase in the presence of random hexamers (all reagents from Thermo Fisher Scientific). The resulting cDNA was brought to a final volume of 100 μL. An aliquot of 3 μL was used to perform quantitative PCR using the Brilliant II SYBR Green Master Mix (Stratagene) and specific primers against MALAT1 or the reference gene 18S (Table 2). Amplification reactions were carried out in a LightCycler 480 qPCR Instrument (Roche). MALAT1 abundancy was determined by the ΔΔCt method.[50]

Table 2 Primers sequences used in this study. All sequences are displayed from 5′ to 3′

Name	Sequence
MALAT1_FW	5′-TGATGAGAACATTATCTGCATATGCC-3′
MALAT1_RV	5′-TGAGATGGACATTGCCTCTTCA-3′
18S_FW	5′-GTAACCCGTTGAACCCCATT-3′
18S_RV	5′-CCATCCAATCGGTAGTAGCG-3′

Fluorescence imaging

Cells grown on glass coverslips were incubated with a FAM-labeled MALAT1-cleaving DNAzyme for 12 h, 24 h or 48 h. The variant used in this experiment is an analogue of the LNA-modified DNAzyme used in the study, labeled with FAM at the 5′ end. An additional T was incorporated to this side of the sequence to avoid the known quenching of fluorescence generated by guanine (see Table 1). Cells were then fixed for 10 min with 4% formaldehyde (Sigma-Aldrich) in 1× phosphate-buffered saline (PBS: 137 mM NaCl, 2.7 mM KCl, 10 mM Na_2HPO_4, 1.8 mM KH_2PO_4). Fixed cells were subsequently incubated with PBS containing 2 drops per mL of NucBlue Fixed Cell ReadyProbes (Thermo Fisher Scientific) to counterstain the nucleus. Finally, coverslips were mounted onto slides using Fluoromount-G (Thermo Fisher Scientific). Images were acquired in a Nikon Eclipse epifluorescence microscope (Japan) controlled by a NIS-Elements software. Further image processing was performed using ImageJ software.

Statistical analyses

Statistical comparisons were performed using GraphPad Prism software. Specific tests are indicated in each figure legend.

Results and discussion

Incorporation of LNA modifications in the substrate recognition region of the 10–23 not only have demonstrated an improvement in stability, in many cases the addition of modifications has also resulted in an increment in the DNAzyme activity.[12,24–26,29] To better explore the influence of this modification on the catalysis of the 10–23, we conducted parallel activity assay under single-turnover condition of the unmodified 10–23 DNAzyme (Fig. 2A and B) and an LNA-modified 10–23 variant (Fig. 2C and D), using Mg^{2+} and Ca^{2+} as cofactors at 2 mM (Fig. 2A–C) and 10 mM concentration (Fig. 2B and D). Table S1† displays the average observed rate constant values obtained for each condition, along with the relative values of the

© 2025 The Author(s). Published by the Royal Society of Chemistry

Open Access Article. Published on 23 April 2025. Downloaded on 4/15/2026 9:26:23 PM.
This article is licensed under a Creative Commons Attribution-NonCommercial 3.0 Unported Licence.

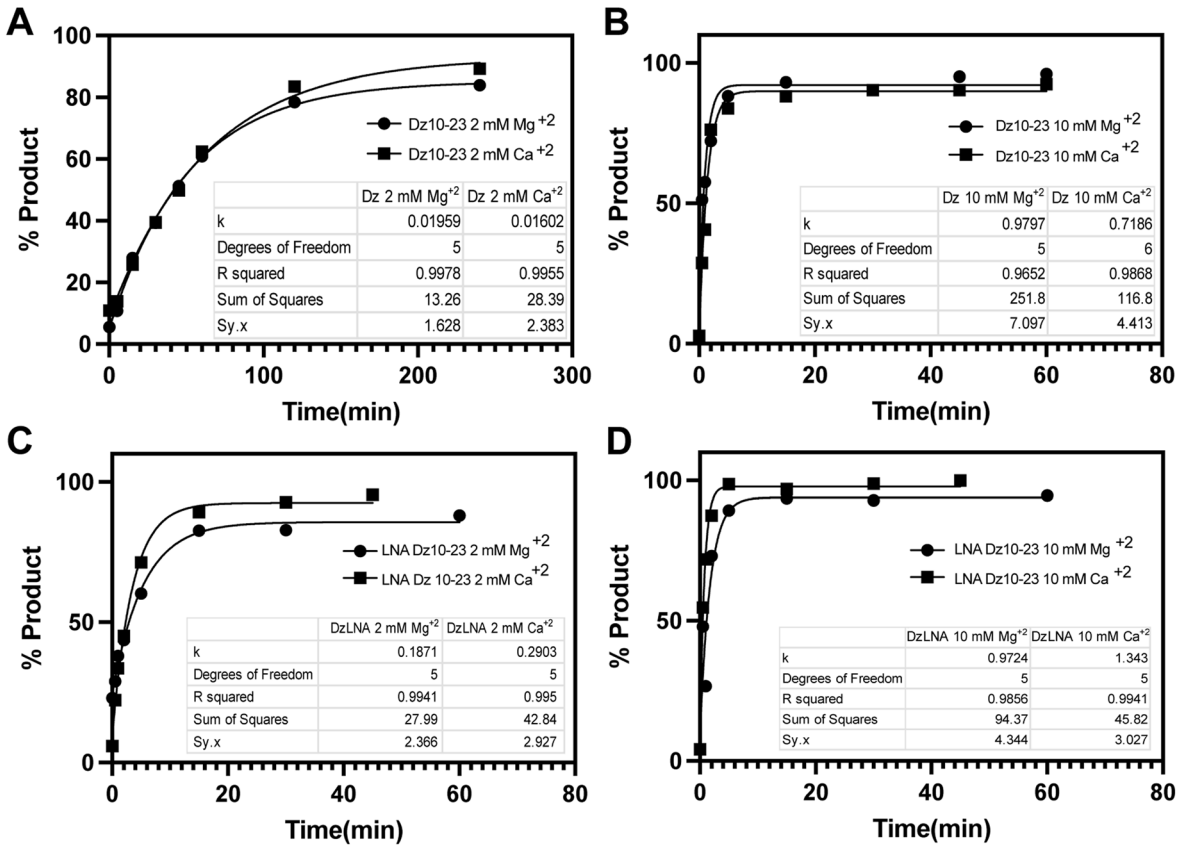

Fig. 2 Representative kinetics of activity assays of the 10–23 DNAzyme (Dz) and the LNA-modified 10–23 (DzLNA) variant with Mg^{2+} (black circles) and Ca^{2+} (black squares). (A) 10–23 DNAzyme with 2 mM M^{2+}. (B) 10–23 DNAzyme with 10 mM M^{2+}. (C) LNA-modified 10–23 variant with 2 mM M^{2+}. (D) LNA-modified 10–23 variant with 10 mM M^{2+}. M^{2+} stands for Mg^{2+} or Ca^{2+}. Results were fitted to eqn (1) (black lines). *k* values and model fit statistics shown enclosed were obtained using Origin 8.5 software.

LNA-modified variant compared to the unmodified DNAzyme at each metal concentration. Representative gels images are shown in Fig. S2.†

The activity assays showed the LNA-modified variant has a higher catalytic activity compared to the unmodified DNAzyme, with a more pronounced and significant effect when Ca^{2+} is used as a cofactor. To facilitate the comparison among the rate constant values for each condition, see box plots displayed in Fig. 3. The observed increment in the activity was particularly notable at 2 mM metal ion concentration (Fig. 3A) compared to 10 mM (Fig. 3B), suggesting that LNA modifications cause a suitable enhance in efficiency, under physiological metal ion concentrations.

LNAs monomers incorporate a ribose ring that is fixed by a methylene bridge connecting the 2′ oxygen and the 4′ carbon.[18] Besides conferring increased stability to nucleases degradation, these unnatural modifications enhances the binding affinity of oligonucleotides to their complementary sequences and restricts the conformational flexibility, making the duplexes structurally constrained.[19] Previous studies have introduced LNA modification within the two binding arms of the 10–23 DNAzyme (inner modifications) to target a stretch of a 58 nt of the *E. coli* 23S rRNA sequence,[26] a 388 nt human EGR-1 transcript,[24] two regions (66 and 67 nt) of the hsa-miR-372 RNA[25] and two highly accessible fragments in the HIV-1. Although some of these studies do not report rate constant values,[24,26] all of them found a substantial increment in the yield of cleavage with the LNA-modified variant after a certain time of incubation (specific to each study). Other studies have explored the effect of adding LNA modification at each end of the binding arms revealing an increased in activity as well, but the extent of enhancement varies among them.[12,29]

Across all the provided examples, the incorporation of LNA modifications consistently increases the activity compared to the unmodified DNAzyme, as we have observed as well, where the introduction of two LNA modifications at each end of the substrate binding domain increased the observed rate constant under single turnover condition, particularly at lower metal ion concentrations. However, correlate the current knowledge on the effect of LNA modifications over the activity is problematic because the reaction rates vary significantly due to the different experimental conditions among studies (Mg^{2+} concentration, temperatures, substrates, *etc.*).[4] Moreover, none of the previous works related the observed increases in activity with the mechanism of catalysis or the specific catalytic strategies employed by the 10–23 DNAzyme.

The recent structural insights suggested that the 10–23 DNAzyme's compacted core region, with an extra turn of the

Open Access Article. Published on 23 April 2025. Downloaded on 4/15/2026 9:26:23 PM.
This article is licensed under a Creative Commons Attribution-NonCommercial 3.0 Unported Licence.

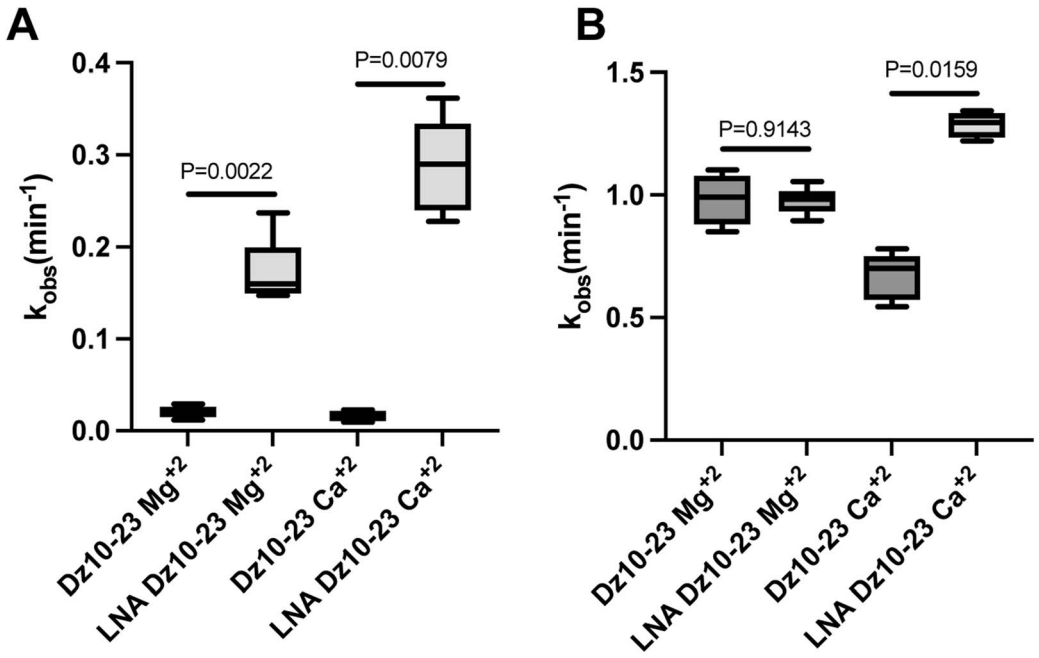

Fig. 3 Box plots of the k_{obs} for the 10–23 DNAzyme (Dz) and the LNA-modified 10–23 (DzLNA) in the presence of (A) 2 mM M^{2+} and (B) 10 mM M^{2+}. M^2 represents Mg^{2+} or Ca^{2+}. *P*-values were obtained using the Mann–Whitney test.

catalytic loop around the RNA, immobilizes the substrate and fully exposes the cleavage site to highly conserved bases,[32] already identified as crucial for catalysis through mutational analysis.[3,47] This configuration, along with the identified metal ion binding regions (Mg^{2+} in the study), supports the in-line conformation needed for the nucleophilic attack.[37] Considering this, and based on our results, it is possible that the structural changes caused by LNA modifications on the DNA:RNA duplex facilitates the proper alignment between the nucleophile (2′-OH), the scissile phosphate, and the leaving group (5′-O), promoting a more effective α-catalysis (see Fig. S1†). Furthermore, the conformational changes induced by the LNAs could also enhance binding affinity,[33] potentially optimizing the alignment of catalytically relevant groups, favoring other catalytic strategies that assist the cleaving reaction already found.[38]

Given that the observed improvement in activity was more significant at lower metal ion concentrations, we examined the influence of metal concentration on the activity of the 10–23 DNAzyme and its LNA-modified variant with Mg^{2+} (Fig. 4A) and Ca^{2+} (Fig. 4B). The changes observed in the dissociation constant (K_D) provide valuable insights into how LNA modifications affect metal ion binding affinity and the activity of the 10–23 DNAzyme. With Mg^{2+}, a slight (but not significant) increase in the K_D value is observed upon introducing the LNA modifications, indicating a small reduction in affinity for Mg^{2+} (Fig. 4A). This might suggest that LNA modifications slightly disrupt the optimal binding environment for Mg^{2+}. Despite this, the catalytic activity of the LNA-modified variant remains higher, suggesting that other factors, such as improved preorganization of the active site, favor the reaction.

With Ca^{2+}, a significant decrease in K_D is observed (Fig. 4B), indicating a markedly higher affinity for Ca^{2+} in the LNA-modified DNAzyme. This suggests that LNA modifications might create a more favorable binding environment for Ca^{2+}, possibly through better coordination or stabilization of the metal ion. The enhanced affinity for Ca^{2+} likely contributes to the observed increment in catalytic activity, especially at lower metal ion concentrations. This improved binding affinity might facilitate the role of the divalent metal ion cofactor in the stabilization of the leaving group during the reaction (δ-catalysis, see Fig. S1†).[38] The increase in catalytic activity by introduction of modifications, particularly at lower concentrations of metal ions, might be attributed to the structural changes imparted by the incorporation of LNAs. At low metal concentrations, where saturation has not yet been reached, the rigidity provided by the LNA could benefit the conformation of the active DNAzyme.

After completing the *in vitro* assays, we evaluated the effectiveness of DNAzymes in modulating the expression of MALAT1 in human cells, performing the subsequent experiments only with the LNA-modified variant based on its higher activity. Prior to conducting cellular studies, we evaluated the impact of the [LNA-Dz] : [S] ratio on the activity of the 10–23. To do this, we performed a dose-response curve, maintaining a constant substrate concentration of 1 μM while varying the DNAzyme concentration (100 nM–25 μM) to test different ratios. The results presented in Fig. 5 indicate a sustained increase in the rate constant with rising DNAzyme concentrations up to a ratio of 5 : 1 ([LNA-Dz] : [S]), forming a plateau afterwards. This trend was observed with 2 mM Mg^{2+} and 2 mM Ca^{2+}, with Ca^{2+} enabling a maximum activity higher than Mg^{2+}, consistent with previous observations.

© 2025 The Author(s). Published by the Royal Society of Chemistry

Open Access Article. Published on 23 April 2025. Downloaded on 4/15/2026 9:26:23 PM.
This article is licensed under a Creative Commons Attribution-NonCommercial 3.0 Unported Licence.

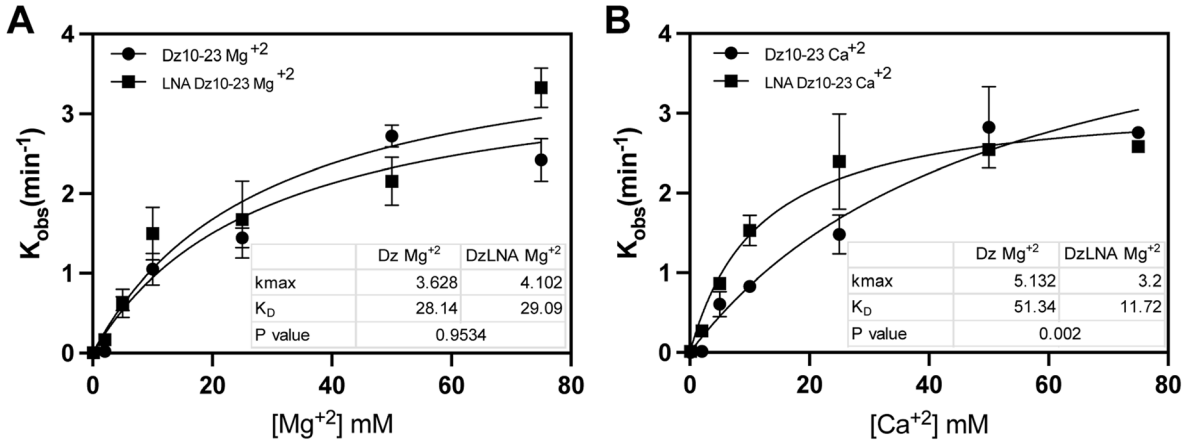

Fig. 4 Influence of the concentration of the divalent metal cofactor on the activity (k_{obs}) of the 10–23 DNAzyme (Dz) and the LNA-modified 10–23 (DzLNA), measured under single-turnover conditions with (A) Mg^{2+} and (B) Ca^{2+}. Results were fitted to eqn (2) (black lines). *P*-values for differences in dissociation constants (K_D) were calculated using the extra sum-of-squares F-test in GraphPad Prism.

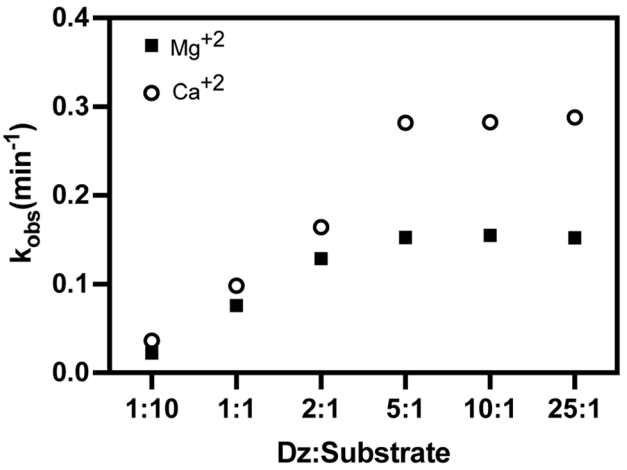

Fig. 5 Influence of the LNA-DNAzyme and the substrate concentrations ratio on the activity (k_{obs}) of the LNA Dz10-23, in presence of 2 mM Mg^{2+} (black square) and Ca^{2+} (white dots). RNA-substrate concentration remained constant at 1 μM in each individual assay.

Cellular studies

Subsequently, cellular assays were performed using the human breast cancer MCF7 cell line. For this, we consider the fact that in live cells, the availability of free ions could limit the function of DNAzymes. The 10–23 DNAzyme can utilize Mg^{2+} and Ca^{2+} ions to promote catalysis.[3] Intracellular concentrations of these ions are tightly regulated. Specifically, basal cytoplasmic calcium levels are typically around 100 nM, but it is stored in the reticulum in the 100 μM–1 mM range.[51] Free magnesium levels (available for biochemical processes) range between 0.1 and 6 mM in animal cells.[52] These ions play critical roles in many cellular processes, and their levels fluctuate dynamically during the cell's life cycle. It is important to consider that an increase in intracellular magnesium tends to suppress calcium levels and *vice versa*.[53] This inverse relationship implies that, for DNAzymes that can utilize both ions as metal ion cofactors, at least one of these ions will typically be available to support the DNAzyme's catalytic activity.

Since MALAT1 is critical for breast cancer cell survival and its depletion may lead to cell death,[41–43] we first performed cell counting following treatment with the DNAzyme targeting MALAT1. After 24 h of incubation with the LNA-modified 10–23, no significant changes in cell viability number were observed compared to a catalytically inactive variant (data not shown). However, after 48 h, a decreasing trend in cell survival was detected at DNAzyme concentrations ranging from 0.5 to 4 μM, specifically with the catalytically active variant (Fig. 6A). MALAT1 expression was reduced to 50% at 0.5 μM 12 h post-transfection but returned to baseline at 24 (Fig. 6B, left). In contrast, at 4 μM, MALAT1 levels gradually decreased from 40% of control levels at 12 h to 20% after 48 h (Fig. 6B, right). Notably, significant cell death was observed after 72 h, preventing a reliable gene expression quantification at this time point. To assess the persistence of the LNA-modified 10–23 DNAzyme in MCF7 cells, we tracked a FAM-labeled variant (Table 1) using epifluorescence microscopy (Fig. 6C). The DNAzyme accumulated in cells as early as 12 h post-transfection, reached maximal levels at 24 h, and then gradually decreased at 48 h and 72 h (Fig. 6C). In summary, our results indicate that the DNAzyme exerts a concentration-dependent and cumulative effect in downregulating MALAT1, ultimately leading to cell death. The observed reduction in DNAzyme levels over time may be attributed to active efflux mechanisms or dilution due to cellular proliferation, consistent with previous reports.[54]

The Chiba group conducted experiments using an 8–17 XNAzyme targeting mouse MALAT1.[45] This XNAzyme incorporated LNA, PS, and 2′-OME modifications, achieving its maximum silencing potential (~50%) at a concentration of 100 nM after 18 hours in mouse Hepa1c1c7 cells. Strikingly, the effect was lost after 48 h and their mutated, catalytically inactive variant also reduced the expression of MALAT1 in ~20%, indicating that additional mechanisms like RNAse H-mediated RNA

Open Access Article. Published on 23 April 2025. Downloaded on 4/15/2026 9:26:23 PM.
This article is licensed under a Creative Commons Attribution-NonCommercial 3.0 Unported Licence.

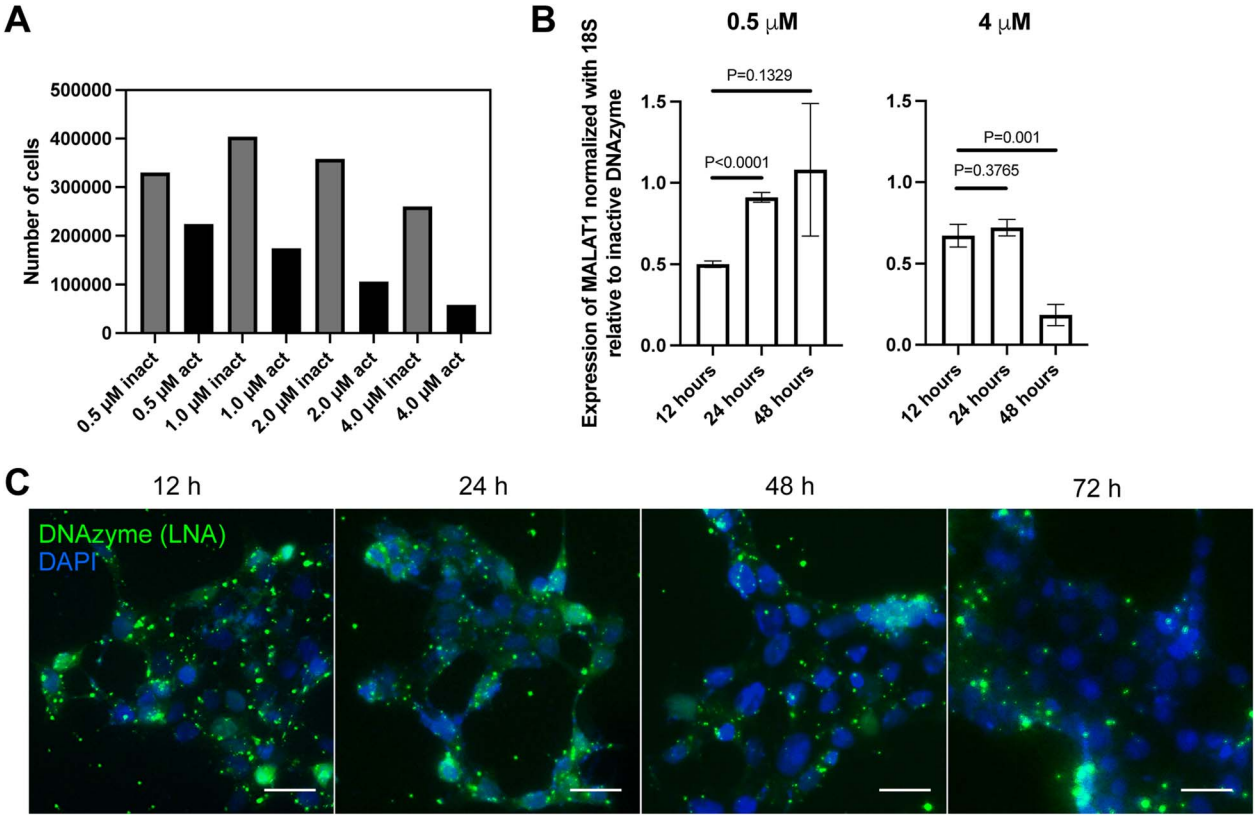

Fig. 6 Evaluation of the LNA-modified 10–23 DNAzyme in MCF7 breast cancer cells. (A) Cells treated with the active LNA modified DNAzyme (black bars) or a catalytically inactive variant (grey bars) were counted after trypsinization using a Neubauer chamber. A representative result of three independent biological replicates is shown. (B) MALAT1 expression quantified using specific primers (Table 2). DNAzyme concentrations and incubation times are indicated in each plot. Housekeeping gene 18S was used for normalization. Results are expressed as mean ± S.D. from three replicates. *P*-values for differences between time points were calculated using Welch's *t*-test in GraphPad Prism. (C) Epifluorescence images of cells transfected with FAM-labeled LNA-modified 10–23 DNAzyme (green). Nuclei are stained with DAPI (blue). Incubation times are indicated at each frame. A representative field is shown from at least four acquired images. Scale bar: 20 μm.

cleavage may be in place.[55] In contrast, our DNAzyme reached 80% of silencing at 48 h with a concentration of 4 μM, with no evidence of RNAse H-mediated mechanism (MALAT1 expression remains unchanged in our catalytically inactive form even after 48 h). Thus, these results indicate that our LNA modified DNAzyme is stable and effective in terms of silencing percentage, as it continues to exhibit significant silencing at 48 h in higher concentrations. Importantly, we have evidence of cell death only with the active DNAzyme, which is expected following MALAT1 silencing in this cancer cell model [41–43].

The relevance of LNA modifications for the *in vitro* activity of DNAzymes was introduced by a seminal report by Vester *et al.* using the *Escherichia coli* 23S ribosomal RNA as target in *in vitro* reactions.[56] Later, in 2004, Fahmy and Khachigian reported the cleavage of human EGR-1, an RNA coding for a protein transcription factor involved in smooth muscle proliferation after injury. In line with our results, by modifying two nucleotides in each of the hybridizing arms substituted with LNA monomers,[57] they found that this modification is sufficient to efficiently knock-down a gene in cells, indicating that two LNAs per arm are adequate to achieve the knock-down. Given the increasing number of non-coding RNAs involved in disease and the promising use of RNAs as therapeutic targets,[14] further studies are needed to evaluate if these findings are applicable to other coding and non-coding RNAs participating in distinct biological processes.[24]

Conclusions

Our findings indicate that introduction of two LNA modifications at the substrate recognition regions of the 10–23 DNAzyme is sufficient to enhance its catalytic efficiency, particularly in the presence of 2 mM Ca^{2+}, rather than 10 mM. Similar results were found with Mg^{2+}. These modifications likely cause structural changes that assist the catalytic strategies used by the 10–23, probably supporting interactions necessary for efficient nucleophile activation, leaving group stabilization or by enhancing metal ion coordination capabilities. Cellular studies showed a 40% of silencing at 12 h and 80% at 48 h with a concentration of 4 μM of the LNA-modified DNAzyme with no evidence of RNAse H-mediated activity, confirming that LNA-modified DNAzymes are promising tools to modulate expression of relevant human transcripts involved in disease. These insights highlight the need of further studies with focus on systematic

© 2025 The Author(s). Published by the Royal Society of Chemistry

Open Access Article. Published on 23 April 2025. Downloaded on 4/15/2026 9:26:23 PM. This article is licensed under a Creative Commons Attribution-NonCommercial 3.0 Unported Licence.

comparisons of various chemical modifications to establish robust guidelines for optimizing DNAzyme design and understanding their mechanistic implications and its comparison with *in vivo* studies, focusing on diseases related RNA targets.

Data availability

The data supporting this article have been included as part of the ESI.†

Author contributions

Conceptualization: RA, AAM, MCP; investigation: MMG, RA, MCP; data analysis: MMG, RA, AAM and MCP; resources: RA, MCP; writing – original draft: MMG, RA, AAM and MCP.

Conflicts of interest

The authors declare no competing conflict of interest.

Acknowledgements

Universidad Andres Bello, Project DI-05-24-REG (MCP); ANID FONDECYT Regular 1240853 (RA)

References

1 S. W. Santoro and G. F. Joyce, *Proc. Natl. Acad. Sci.*, 1997, **94**, 4262–4266.
2 S. W. Santoro and G. F. Joyce, *Biochemistry*, 1998, **37**, 13330–13342.
3 H. Rosenbach, J. Victor, M. Etzkorn, G. Steger, D. Riesner and I. Span, *Molecules*, 2020, **25**, 3100.
4 J. Yan, M. Ran, X. Shen and H. Zhang, *Adv. Mater.*, 2023, **35**, 2300374.
5 N. Krug, J. M. Hohlfeld, A.-M. Kirsten, O. Kornmann, K. M. Beeh, D. Kappeler, S. Korn, S. Ignatenko, W. Timmer, C. Rogon, J. Zeitvogel, N. Zhang, J. Bille, U. Homburg, A. Turowska, C. Bachert, T. Werfel, R. Buhl, J. Renz, H. Garn and H. Renz, *N. Engl. J. Med.*, 2015, **372**, 1987–1995.
6 Y. Cao, L. Yang, W. Jiang, X. Wang, W. Liao, G. Tan, Y. Liao, Y. Qiu, D. Feng, F. Tang, B. L. Hou, L. Zhang, J. Fu, F. He, X. Liu, W. Jiang, T. Yang and L.-Q. Sun, *Mol. Ther.*, 2014, **22**, 371–377.
7 G. Grassi and M. Grassi, *The Lancet*, 2013, **381**, 1797–1798.
8 E.-A. Cho, F. J. Moloney, H. Cai, A. Au-Yeung, C. China, R. A. Scolyer, B. Yosufi, M. J. Raftery, J. Z. Deng, S. W. Morton, P. T. Hammond, H.-T. Arkenau, D. L. Damian, D. J. Francis, C. N. Chesterman, R. S. C. Barnetson, G. M. Halliday and L. M. Khachigian, *The Lancet*, 2013, **381**, 1835–1843.
9 C. R. Dass and P. F. M. Choong, *Oligonucleotides*, 2010, **20**, 51–60.
10 V. Popp, K. Gerlach, S. Mott, A. Turowska, H. Garn, R. Atreya, H.-A. Lehr, I. C. Ho, H. Renz, B. Weigmann and M. F. Neurath, *Gastroenterology*, 2017, **152**, 176–192.
11 K. Nguyen, T. N. Malik and J. C. Chaput, *Nat. Commun.*, 2023, **14**, 2413.
12 Y. Wang, K. Nguyen, R. C. Spitale and J. C. Chaput, *Nat. Chem.*, 2021, **13**, 319–326.
13 A. A. Fokina, D. A. Stetsenko and J.-C. François, *Expet Opin. Biol. Ther.*, 2015, **15**, 689–711.
14 R. Aguilar, C. Mardones, A. A. Moreno and M. Cepeda-Plaza, *FEBS J.*, 2025, DOI: **10.1111/febs.17368**.
15 R. Bhindi, R. G. Fahmy, H. C. Lowe, C. N. Chesterman, C. R. Dass, M. J. Cairns, E. G. Saravolac, L.-Q. Sun and L. M. Khachigian, *Am. J. Pathol.*, 2007, **171**, 1079–1088.
16 N. Zhang, *Neural Regener. Res.*, 2022, **17**, 1989–1990.
17 P. Sun, H. Gou, X. Che, G. Chen and C. Feng, *Chem. Commun.*, 2024, **60**, 10805–10821.
18 S. Obika, D. Nanbu, Y. Hari, K.-i. Morio, Y. In, T. Ishida and T. Imanishi, *Tetrahedron Lett.*, 1997, **38**, 8735–8738.
19 B. Vester and J. Wengel, *Biochemistry*, 2004, **43**, 13233–13241.
20 P. H. Hagedorn, R. Persson, E. D. Funder, N. Albæk, S. L. Diemer, D. J. Hansen, M. R. Møller, N. Papargyri, H. Christiansen, B. R. Hansen, H. F. Hansen, M. A. Jensen and T. Koch, *Drug Discov. Today*, 2018, **23**, 101–114.
21 C. Zhu, J. Y. Lee, J. Z. Woo, L. Xu, X. Nguyenla, L. H. Yamashiro, F. Ji, S. B. Biering, E. Van Dis, F. Gonzalez, D. Fox, E. Wehri, A. Rustagi, B. A. Pinsky, J. Schaletzky, C. A. Blish, C. Chiu, E. Harris, R. I. Sadreyev, S. Stanley, S. Kauppinen, S. Rouskin and A. M. Näär, *Nat. Commun.*, 2022, **13**, 4503.
22 M. Petersen and J. Wengel, *Trends Biotechnol.*, 2003, **21**, 74–81.
23 M. Chakravarthy, M. T. Aung-Htut, B. T. Le and R. N. Veedu, *Sci. Rep.*, 2017, **7**, 1613.
24 R. G. Fahmy and L. M. Khachigian, *Nucleic Acids Res.*, 2004, **32**, 2281–2285.
25 V. M. Jadhav, V. Scaria and S. Maiti, *Angew. Chem., Int. Ed.*, 2009, **48**, 2557–2560.
26 B. Vester, L. B. Lundberg, M. D. Sørensen, B. R. Babu, S. Douthwaite and J. Wengel, *J. Am. Chem. Soc.*, 2002, **124**, 13682–13683.
27 M. R. Jakobsen, J. Haasnoot, J. Wengel, B. Berkhout and J. Kjems, *Retrovirology*, 2007, **4**, 29.
28 T. C. Roberts, R. Langer and M. J. A. Wood, *Nat. Rev. Drug Discovery*, 2020, **19**, 673–694.
29 S. Schubert, D. C. Gül, H. P. Grunert, H. Zeichhardt, V. A. Erdmann and J. Kurreck, *Nucleic Acids Res.*, 2003, **31**, 5982–5992.
30 L. Robaldo, J. M. Montserrat and A. M. Iribarren, *Bioorg. Med. Chem. Lett.*, 2010, **20**, 4367–4370.
31 L. Robaldo, F. Izzo, M. Dellafiore, C. Proietti, P. V. Elizalde, J. M. Montserrat and A. M. Iribarren, *Bioorg. Med. Chem.*, 2012, **20**, 2581–2586.
32 J. Borggräfe, J. Victor, H. Rosenbach, A. Viegas, C. G. W. Gertzen, C. Wuebben, H. Kovacs, M. Gopalswamy, D. Riesner, G. Steger, O. Schiemann, H. Gohlke, I. Span and M. Etzkorn, *Nature*, 2022, **601**, 144–149.
33 K. Bondensgaard, M. Petersen, S. K. Singh, V. K. Rajwanshi, R. Kumar, J. Wengel and J. P. Jacobsen, *Chem.–Eur. J.*, 2000, **6**, 2687–2695.

© 2025 The Author(s). Published by the Royal Society of Chemistry

Open Access Article. Published on 23 April 2025. Downloaded on 4/15/2026 9:26:23 PM.
This article is licensed under a Creative Commons Attribution-NonCommercial 3.0 Unported Licence.

34 L. M. Larcher, I. L. Pitout, N. P. Keegan, R. N. Veedu and S. Fletcher, *Nucleic Acid Ther.*, 2023, **33**, 178–192.
35 M. J. Cairns, A. King and L. Q. Sun, *Nucleic Acids Res.*, 2003, **31**, 2883–2889.
36 R. R. Breaker, G. M. Emilsson, D. Lazarev, S. Nakamura, I. J. Puskarz, A. Roth and N. Sudarsan, *RNA*, 2003, **9**, 949–957.
37 J. Borggräfe, C. G. W. Gertzen, A. Viegas, H. Gohlke and M. Etzkorn, *FEBS J.*, 2023, **290**, 2011–2021.
38 V. Parra-Meneses, V. Silva-Galleguillos and M. Cepeda-Plaza, *Org. Biomol. Chem.*, 2024, **22**, 6833–6840.
39 N. Amodio, L. Raimondi, G. Juli, M. A. Stamato, D. Caracciolo, P. Tagliaferri and P. Tassone, *J. Hematol. Oncol.*, 2018, **11**, 63.
40 G. Arun and D. L. Spector, *RNA Biol.*, 2019, **16**, 860–863.
41 F. A. Abulwerdi, W. Xu, A. A. Ageeli, M. J. Yonkunas, G. Arun, H. Nam, J. S. Schneekloth Jr, T. K. Dayie, D. Spector, N. Baird and S. F. J. Le Grice, *ACS Chem. Biol.*, 2019, **14**, 223–235.
42 S. Hajibabaei, N. Nafissi, Y. Azimi, R. Mahdian, F. Rahimi-Jamnani, V. Valizadeh, M. H. Rafiee and M. Azizi, *Sci. Rep.*, 2023, **13**, 8652.
43 G. Arun, S. Diermeier, M. Akerman, K. C. Chang, J. E. Wilkinson, S. Hearn, Y. Kim, A. R. MacLeod, A. R. Krainer, L. Norton, E. Brogi, M. Egeblad and D. L. Spector, *Genes Dev.*, 2016, **30**, 34–51.
44 F. Khani-Habibabadi, L. Zare, M. A. Sahraian, M. Javan and M. Behmanesh, *Mol. Neurobiol.*, 2022, **59**, 4209–4222.
45 K. Chiba, T. Yamaguchi and S. Obika, *Chem. Sci.*, 2023, **14**, 7620–7629.
46 N. Amodio, M. A. Stamato, G. Juli, E. Morelli, M. Fulciniti, M. Manzoni, E. Taiana, L. Agnelli, M. E. G. Cantafio, E. Romeo, L. Raimondi, D. Caracciolo, V. Zuccala, M. Rossi, A. Neri, N. C. Munshi, P. Tagliaferri and P. Tassone, *Leukemia*, 2018, **32**, 1948–1957.
47 Z. a. Zaborowska, J. P. Fürste, V. A. Erdmann and J. Kurreck, *J. Biol. Chem.*, 2002, **277**, 40617–40622.
48 C. Cortés-Guajardo, F. Rojas-Hernández, R. Paillao-Bustos and M. Cepeda-Plaza, *Org. Biomol. Chem.*, 2021, **19**, 5395–5402.
49 Q.-C. He, J.-M. Zhou, D.-M. Zhou, Y. Nakamatsu, T. Baba and K. Taira, *Biomacromolecules*, 2002, **3**, 69–83.
50 K. J. Livak and T. D. Schmittgen, *Methods*, 2001, **25**, 402–408.
51 D. Eisner, E. Neher, H. Taschenberger and G. Smith, *Physiol. Rev.*, 2023, **103**, 2767–2845.
52 G. M. Walker, *Crit. Rev. Biotechnol.*, 1994, **14**, 311–354.
53 A. Zhang, T. P. O. Cheng and B. M. Altura, *Biochim. Biophys. Acta, Mol. Cell Res.*, 1992, **1134**, 25–29.
54 Y. Liu, S. Zhang, M. Zhang, X. Liu, Y. Wu, Q. Wu, J. C. Chaput and Y. Wang, *Nucleic Acids Res.*, 2025, **53**(5), DOI: **10.1093/nar/gkaf144**.
55 A. I. Taylor and P. Holliger, *Nat. Chem.*, 2022, **14**, 855–858.
56 B. Vester, L. B. Lundberg, M. D. Sorensen, B. R. Babu, S. Douthwaite and J. Wengel, *J. Am. Chem. Soc.*, 2002, **124**, 13682–13683.
57 R. G. Fahmy and L. M. Khachigian, *Nucleic Acids Res.*, 2004, **32**, 2281–2285.

© 2025 The Author(s). Published by the Royal Society of Chemistry